Clays and Clay Minerals, Vol. 60, No. 4, 341–347, 2012.

FIRST-PRINCIPLES MOLECULAR DYNAMICS INSIGHT INTO Fe^{2+} COMPLEXES ADSORBED ON EDGE SURFACES OF CLAY MINERALS

XIANDONG LIU[1,*], EVERT JAN MEIJER[2], XIANCAI LU[1], AND RUCHENG WANG[1]

[1] State Key Laboratory for Mineral Deposits Research, School of Earth Sciences and Engineering, Nanjing University, Nanjing 210093, P.R. China

[2] Van't Hoff Institute for Molecular Sciences and Amsterdam Centre for Multiscale Modelling, University of Amsterdam, Nieuwe Achtergracht 166, 1018 WV Amsterdam, The Netherlands

Abstract—Using first-principles molecular-dynamics simulations, probable inner-sphere complexes of Fe^{2+} adsorbed on the edge surfaces of clay minerals were investigated. Ferrous ions are important reductants in natural processes and their properties can be altered significantly by complexation on edge surfaces of clay minerals. However, the microscopic picture of adsorption sites and structures of Fe^{2+} is difficult to reveal with modern experimental techniques and, therefore, remains unclear. From the results of first-principles molecular-dynamics simulations, evidence has been provided that complexes on $\equiv$Si$-$O sites were the most stable forms, which should be responsible for the experimentally observed pH-dependent uptake. Such complexation was found to be strong enough to distort the local coordination structures of Si-O tetrahedra in the substrate. Analyses showed that $Fe^{2+}-O_{water}$ coordination structures were dominated by the solvent with surface groups participating in the complexes *via* H bonding. The present study provided a microscopic basis for understanding the chemical processes involving surface-complexed Fe^{2+} ions.

Key Words—Complexation, Edge Surface, Ferrous Ion, First-principles Molecular Dynamics, Hydration.

INTRODUCTION

Fe^{2+} is an important reductant in semi-anoxic and anoxic environments and the Fe^{2+}/Fe^{3+} couple plays central roles in many geochemical and biochemical processes in nature (Murad and Fischer, 1988; Grenthe *et al.*, 1992; Charlet *et al.*, 1998; Fredrickson *et al.*, 2004; Hofstetter *et al.*, 2006; Peretyazhko *et al.*, 2008; Um *et al.*, 2011). The 2:1 type clay minerals, which are ubiquitous in soils and sediments and which have large specific surface areas and porosities, are the major substrates adsorbing metal ions in various environments (Sposito *et al.*, 1999; Bergaya *et al.*, 2006). These phyllosilicates constitute an important pool in the global Fe cycle; they contain Fe as structural ions and also bind cations by surface adsorption (Stucki, 2006). Adsorption can influence the properties of Fe^{2+}. For example, Gehin *et al.* (2007) observed pH-dependent adsorption and reversible oxidation of aqueous Fe^{2+} in the presence of a synthetic Fe-free montmorillonite. In contrast, Peretyazhko *et al.* (2008) found that Fe^{2+} adsorbed in phyllosilicates showed similar reducing capacity to free cations in the reduction reaction of Tc(VII), but complexation on hematite and goethite increased the reducing reactivity of Fe^{2+} significantly (Peretyazhko *et al.*, 2008; Um *et al.*, 2011). This implied that surface-complexed ferrous iron can be used to reduce some contaminants and thus effectively immobilize them (Peretyazhko *et al.*, 2008; Um *et al.*, 2011). The presence of Fe also impacts the physical properties, structures, and surface reactivity of clays (Stucki, 2006).

At present, no accurate molecular picture of the complexation mechanisms of Fe^{2+} on clay surfaces exists because of the complicated surface structures of the clay minerals. The surface area of 2:1-type clay minerals has contributions from both interlayer (001) and edge (010) and (110) surfaces (White and Zelazny, 1988; Bleam, 1993). Numerous studies have investigated the structures and properties of interlayer surfaces (*e.g.* Cygan *et al.*, 2004, 2009; Bergaya *et al.*, 2006; Liu and Lu, 2006, 2008a; Anderson *et al.*, 2010) and adsorption on these surfaces is widely accepted as being by means of cation exchange.

In contrast, the structures of edge surfaces are much more complex and, thus, their properties are more subtle. At these surfaces, many broken bonds are present and, under ambient conditions, they are usually saturated by chemically adsorbed water molecules (Lagaly, 2006; Churakov, 2006, 2007). Recently, first-principles molecular-dynamics (FPMD) simulations were employed to quantify the structures of interfaces between edge surfaces and water (Liu *et al.*, 2012). Detailed H-bond analyses indicated that edge surface groups, including $\equiv$Si$-$OH, $\equiv$Al$-$OH, and $\equiv$Mg$-$OH, perform as both proton donors and acceptors. This leads to the surface acid/base reactivity of clay minerals. Due to the amphotericity of surface groups, edge surfaces bind ions mainly through complexation, which can be rather

* E-mail address of corresponding author:
xiandongliu@nju.edu.cn
DOI: 10.1346/CCMN.2012.0600401

complicated (White and Zelazny, 1988; Bleam, 1993; Sposito *et al.*, 1999). For example, experiments have shown that Fe^{2+} adsorption was almost constant for pH<6.75 when the cation exchange process occurring on interlayer surfaces dominated; for pH >6.75, the adsorption showed a dramatic increase with the advent of complexation at edge sites (Schultz and Grundl, 2004; Jaisi *et al.*, 2008). They also showed that the complexation stage could be fit by a single adsorption affinity (Schultz and Grundl, 2004). However, the molecular-level mechanisms are completely unknown, *e.g.* which surface sites are involved, whether only one or several sites operate, and what do the complexes look like? Indeed, revealing these aspects is not feasible, even by state-of-the-art EXAFS (Extended X-ray Absorption Fine Structure). This is due to the irregularity of edge surfaces and the similar bond lengths of surface groups, such as ≡Al−O and ≡Si−O (Den Auwer *et al.*, 2003; Denecke, 2006).

In the present study, the FPMD technique (Car and Parrinello, 1985; CPMD, 2001) was employed to investigate Fe^{2+} complexed on the edge surfaces of clay minerals. All possible complexation edge sites were taken into account: ≡Si−O and ≡Al−O on (010); ≡Si−O and ≡Al−O−Si≡ on (110). Incorporating explicit water molecules ensured that the role of water was modeled accurately. The fluctuations due to thermal motion were noted properly, as MD was used for simulations. The present study identified ≡Si−O sites as the dominant complexation sites. The findings in this study constitute the first accurate molecular picture of Fe^{2+} adsorption on edge surfaces, and form a basis for a better understanding of the chemical processes involving surface-adsorbed Fe^{2+} as a reductant.

METHODOLOGY

The models

The model clay structure was derived from Viani *et al.* (2002). The chemical formula was $Al_4Si_8O_{20}(OH)_4$ and the crystallographic parameters were a = 5.18 Å, b = 8.98 Å, c = 10 Å, and $\alpha = \beta = \gamma = 90°$. No isomorphic substitution was imposed in the clay layer. For phyllosilicates, the periodic bond chain (PBC) theory (Hartman and Perdock, 1955abc) predicted the edge surfaces of (010) and (110) types (White and Zelazny, 1988; Bickmore *et al.*, 2003). The edge structures were cut from the unit cell and repeated along the a axis, and thus two unit cells were contained in the simulated models. The ≡Al−O−Si≡ and ≡Si−O−Si≡ sites on (010) and the ≡Si−O−Si≡ and ≡Al−O−Al≡ sites on (110) are hidden from the solution due to the irregular interfaces and do not interact with the solution (Churakov, 2006). Therefore, the possible complexation surface sites include: ≡Si−O and ≡Al−O on (010); and ≡Si−O and ≡Al−O−Si≡ on (110). For the initial edge models, the dangling Si−O and Al−O bonds were all saturated with protons (Churakov, 2006, 2007; Liu *et al.*, 2008b, 2012). Each edge model contained 92 atoms.

Each model was placed in a 3D, periodically repeated box which had side lengths of 10.36 Å, 22 Å, and 10 Å, *i.e.* a solution space of ~12 Å was present in the direction vertical to the edge surface. The initial configuration was built for each potential complexation site. Because this study focused on the complexation site and complex structure, rather than on the adsorption process, the ferrous cation was initially placed near the complexation site. For the system where ≡Si−O or ≡Al−O served as a complexation site, the proton was removed from the initial surface group (*i.e.* ≡Si−OH or ≡Al−OH), and then Fe^{2+} was placed ~2.5 Å away from the dangling O (this distance was taken from the $Fe^{2+}-O_{water}$ radial distribution function (RDF) in aqueous solutions) (Herdman and Neilson, 1992). In the (110) ≡Al−O−Si≡ system, Fe^{2+} was placed at a similar distance. For each box, 36 water molecules were inserted into the solution space and this corresponded approximately to the bulk water density: five 1^{st}-shell waters were placed around the cation according to the previous study (Herdman and Neilson, 1992) and the other water molecules were placed randomly.

Computational details

The simulations were performed using the CPMD package (CPMD-3.11.1, 2001). Density functional theory was used to calculate the electronic structures, deploying the BLYP function (Becke, 1988; Lee *et al.*, 1988). Norm-conserving Martins-Trouillier pseudopotentials (Troullier and Martins, 1991) and the Kleinman-Bylander scheme (Kleinman and Bylander, 1982) were used to describe the interactions between the valence and the core states. Wave functions were expanded in a plane wave basis set and the kinetic energy cutoff was set at 90 Ry, which ensured a reasonable convergence of the total energy. For all simulations, a periodic boundary condition was applied. The charges of the systems were compensated by a neutralizing background charge in the simulations.

By assigning to hydrogen a mass of deuterium, the equation of motion was integrated with a time step of 0.168 fs and the fictitious electronic mass was set to 1200 a.u., which maintained the adiabatic conditions. The temperature was set at 300 K and controlled with the Nosé-Hoover thermostat. After the equilibration simulations of ~10−15 ps, production simulations were performed for over 14 ps and statistics were collected every four time steps.

RESULTS AND DISCUSSIONS

Representative snapshots (Figure 1) of edge-complexed Fe^{2+} ions were taken from equilibrated configurations. For the complexes involving both ≡Si−O sites and the ≡Al−O−Si≡ site, the equilibrated configura-

https://doi.org/10.1346/CCMN.2012.0600401 Published online by Cambridge University Press

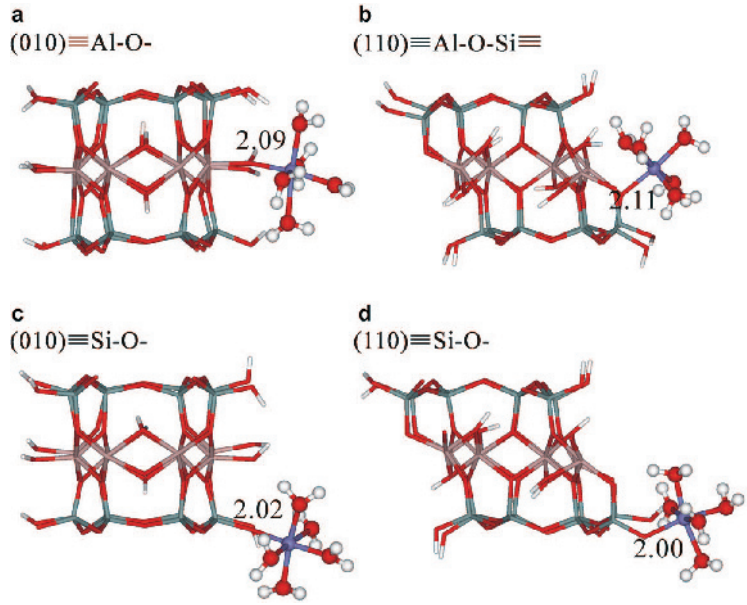

Figure 1. Representative snapshots of the simulated complexes. Substrates are shown as sticks: O = red, H = clear, Si = gray, and Al = pink; complexes are shown as ball-stick models: O = red, H = clear, and Fe = dark gray. The numbers denote the $Fe-O_{edge}$ bond lengths (Å). For clarity, the water molecules not directly coordinated to Fe^{2+} are not shown.

tions were formed in a gradual manner, showing no reactive events on the timescale of the simulations. In contrast, in the simulation of the complexation of Fe^{2+} to the $\equiv Al-O$ site, a series of proton-transfer events occurred: the complex evolved from $\equiv Al-O\text{-}Fe(H_2O)_5^{2+}$ *via* $\equiv Al-_HO-Fe(H_2O)_4(OH)^+$ to $\equiv Al-_HO-Fe(H_2O)_5^{2+}$. After equilibration of the initial configuration, a proton transferred from an Fe^{2+}-coordinated water to the bridging O of $\equiv Al-O-Fe$. This yielded an edge-surface hydroxyl group (Figure 2b, left and middle). Note that during the initial equilibration simulation, the O–H bond lengths of the coordinated waters were fixed, keeping the water ligands intact and allowing the system to equilibrate. The trajectories of $Fe-O_{edge}$ and $H-O_{edge}$ bond length (Figure 2) illustrate that proton-transfer begins once the constraint is removed at ~12 ps. The curve (Figure 2) also shows that, upon protonation of the edge oxygen, the $Fe-O_{edge}$ bond elongated from 2.0 to 2.1 Å. Subsequently, after ~1 ps, a proton transferred from a solvent water to the deprotonated Fe^{2+} coordinated water (Figure 2b, middle and right). These observations indicated that the initial $\equiv Al-O-Fe(H_2O)_5^{2+}$ configuration, with a deprotonated edge hydroxyl group, was unstable.

The edge oxygens in complexes with $\equiv Al-OH$ (evolved from $\equiv Al-O$ as described above) and $\equiv Al-O-Si\equiv$ sites (Figure 1a,b) had a similar chemical environment, both forming two single bonds with neighboring atoms. Therefore, the interactions between Fe^{2+} and edge O were similar, explaining why the average $Fe-O_{edge}$ bond lengths were similar (2.1 Å). For both other complexes, involving the $\equiv Si-O$ sites, the surface oxygens were singly bonded (dangling). This gave rise to a stronger interaction with the complexed Fe^{2+}, resulting in a shorter $Fe-O_{edge}$ bond length of ~2.0 Å. Actually, the immediate elongation of the $Fe-O_{edge}$ bond shown (Figure 2a) gave the impression of bond weakening associated with the protonation of the bridging oxygen.

Next, the strengths of Fe^{2+} complexation and the complexation-induced structural modifications of the substrate were quantified; the pair distribution functions (PDFs) of internal metal–O pairs of the Fe^{2+}-complexed polyhedron were compared with the counterpart PDFs in the non-complexed unit cell (Figure 3). The comparison for the more weakly complexed $\equiv Al-OH$ and $\equiv Al-O-Si\equiv$ sites (Figures 3a,b) showed almost superimposed PDFs, indicating that the internal substrate structure was scarcely influenced by Fe^{2+} complexation. In contrast, the apparent extensions of Si–O bonds (Figure 3c,d) indicated that the relatively strong Fe^{2+} complexation with both $\equiv Si-O$ sites induced a significant weakening of the internal Si–O interactions.

The Fe^{2+}-water coordination for $\equiv Al-OH$ and $\equiv Al-O-Si\equiv$ complexed structures was characterized by an average $Fe^{2+}-O_{water}$ distance of 2.02 Å (Figure 4). Fe^{2+} had a weak Jahn-Teller effect and for aqueous $Fe(H_2O)_6^{2+}$ the Fe–O distance range was ~2.02–2.10 Å. Therefore, the value of 2.02 Å is at the lower edge (Herdman and Neilson, 1992; Ensing and Baerends, 2002; Ensing *et al.*, 2002; Remsungnen and Rode, 2003; Amira *et al.*, 2004). The $Fe-O_{edge}$ bond length of 2.10 Å for these two complexes was significantly longer (Figures 1a,b), indicating that Fe^{2+} may favor complete solvation over binding with the $\equiv Al-OH$ and $\equiv Al-O-Si\equiv$ surface sites. By recalling the

https://doi.org/10.1346/CCMN.2012.0600401 Published online by Cambridge University Press

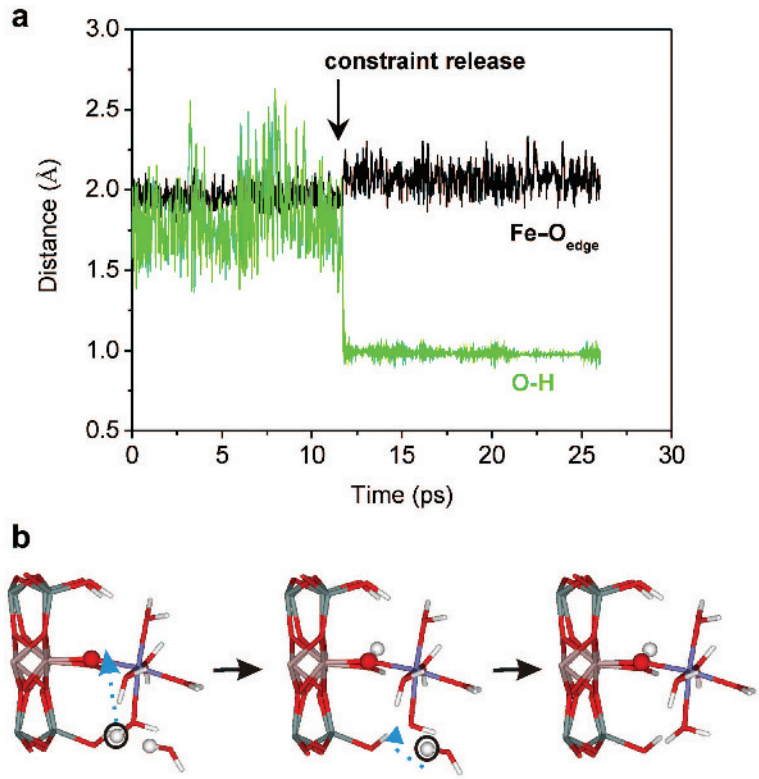

Figure 2. Proton-transfer events in the simulation of the (010) ≡Al−O site system. (a) Time evolutions of O...H bond lengths (acceptor O and leaving H involved in the first proton-transfer event) as shown in part b (left) and Fe−O_{edge} bond lengths. (b) Snapshots showing the two proton-transfer events: (left) the first proton transfer, which was from a coordinated water molecule to the surface O; (middle) the second proton transfer which was from a solvent water molecule to the OH^- ligand; (right) the final configuration. The gray circles denote the transferring protons and the arrows indicate the transfer directions. O = red, H = clear, Si = gray, Al = pink, and Fe = dark gray.

experimental finding of the single complexation affinity (Schultz and Grundl, 2004), this observation and modifications of internal substrate structures strongly suggested that the ≡Si−O site (on both surface planes) was the only active surface site involved in pH-dependent adsorption.

The solvation of ≡Si−O-Fe^{2+} complexes was quantified (Figure 5). The Fe^{2+}−O_{water} RDFs (panel a) for both complexes were similar: a well defined first peak ranging from 1.8 to ~2.3 Å and maximized at 2.02 Å. The second solvation shell appeared as a less pronounced peak at ~3.6−4.5 Å. The distances observed agreed with neutron diffraction data (Herdman and Neilson, 1992) and simulations of Fe^{2+} in bulk aqueous solutions (Ensing and Baerends, 2002; Ensing *et al.*, 2002; Remsungnen and Rode, 2003; Amira *et al.*, 2004).

The snapshots (panels c−d) showed the trigonal leaf structures with the second-shell ligands forming acceptor H bonds from the first-shell water. This is typical for hydrations of multiple-valence cations (Bylaska *et al.*, 2007). The H bonds among the first and second solvation shell (Figure 2b) showed the H−O RDFs and CNs involving the hydrogens of the Fe^{2+} coordinated waters (H_{1st}). The CNs up to 2.5 Å were <1, due to participation of some surface groups in H bonding to the coordinated waters (panels c−d). The difference of the local surface structure for the two ≡Si−O sites implied that H_{1st} on (110) donated, on average, fewer H bonds to the surface than did (010). The snapshots illustrated that two H bonds were donated to surface oxygen on (110) (panel c) and four on (010) (panel d). Overall, these observations showed that the hydration of complexed Fe^{2+} was dominated by the solvent, as it resembled the structures in bulk solution. The presence of surfaces did not give rise to large structural changes, although they participated in the coordination *via* H bonding and, thus, actually served in the role of ligands.

Similar to Fe^{2+} adsorption, experimental measurements of other transition metal cations (*e.g.* Ni^{2+}, Zn^{2+}, Cd^{2+}, Pb^{2+}, Cu^{2+}) also showed an obvious pH-dependent adsorption stage, which was believed to be inner-sphere complexation on clay-edge sites (Baeyens and Bradbury, 1997a, 1997b; Ikhsan *et al.*, 2005; Gu and Evans, 2007, 2008; Gu *et al.*, 2010). Bradbury and Baeyens (1997) employed a modeling approach with no electrostatics to fit the titration curves with two complexation sites (Morel, 1997). However, recent works using approaches with electrostatics showed that the data can be

https://doi.org/10.1346/CCMN.2012.0600401 Published online by Cambridge University Press

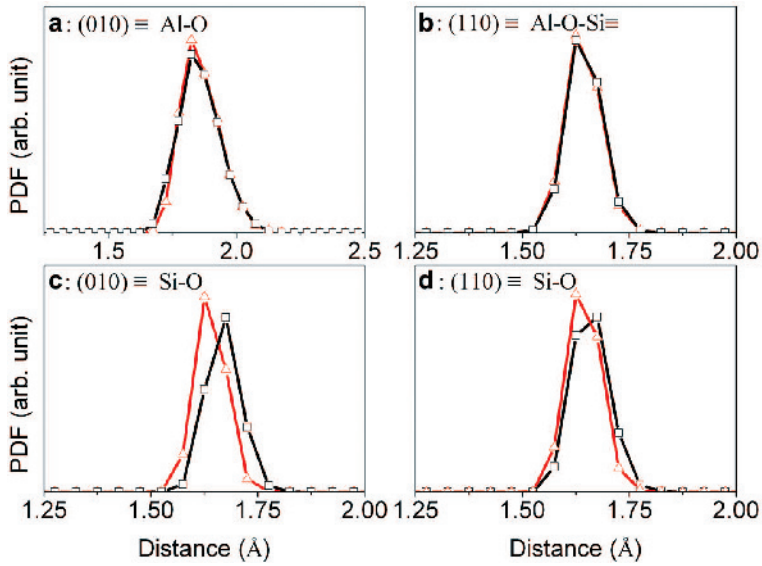

Figure 3. Metal−oxygen pair distribution functions (PDFs) of the polyhedrons in the substrates. Black line = metal−oxygen PDF of the tetrahedron or octahedron on which Fe^{2+} was complexed; red line = PDF of the counterpart polyhedron on the other unit cell. To focus on the inner metal−O coordination structures, only the Si−O and Al−O bonds in substrates were included in the PDF calculations and the surface Si−O or Al−O were discarded; *e.g.* for the complex shown in Figure 1a, the Al−O bond of $\equiv Al-_{H}O-Fe(H_2O)_5^{2+}$ was not included and the Al−O bond of ≡Al−O(H) on the counterpart octahedron on the other cell was not taken into account either.

interpreted very well with a single complexation affinity (*e.g.* Ikhsan *et al.*, 2005; Gu and Evans, 2007, 2008; Gu *et al.*, 2010). Morel (1997) commented in detail on the approach of Bradbury and Baeyens (1997) and showed that an electrostatics term allows fitting of the three important features: the dependence of acid titration on ionic strength, the smoothness of acid titration curves, and the independence of cation adsorption on ionic strength. From the electronic structures viewpoint, these metal cations all have d-shells and their interactions with surface oxygen sites could be similar to the case of ferrous ions. This is one microscopic origin of the similar adsorption characteristics of transition metal cations. One may, therefore, expect that their microscopic mechanisms resemble, to some extent, those of Fe^{2+}; and, with the finding of this study, ≡Si−O may also be the major complexation site for other transition metal cations. An unambiguous understanding of the adsorption mechanisms of those metal cations requires interaction between experiments, experiment-based modeling, and molecular-level simulations. To this end, FPMD simulation provided valuable microscopic and thermodynamic information because of the accurate treatment of both chemical bonding and solvent effects. However, few FPMD studies of these complex interface systems have been carried out.

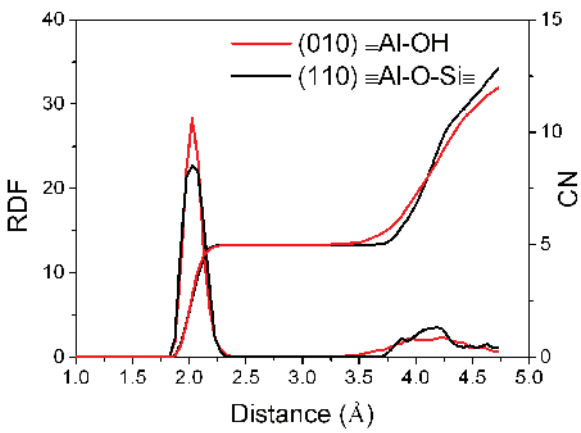

Figure 4. RDF (radial distribution function) and CN (coordination number) for $Fe^{2+}-O_{water}$ in the complexes on (010) ≡Al−OH and (110) ≡Al−O−Si≡ sites.

CONCLUSIONS

Considering that the model mineral used is the prototype for 2:1 phyllosilicates, the finding that Fe^{2+} complexes favored ≡Si−O sites may be generally valid for the whole family of natural phyllosilicates, *e.g.* smectites and micas (Sposito, 1984). This provided a physical basis for understanding other properties and behaviors associated with complexation in both the laboratory and nature, such as reducing capacity, surface precipitation, and growth of Fe-containing phases. Complexation is a precursor process for surface precipitation, so one can expect that precipitation preferentially starts from the edges of the tetrahedral sheets. Furthermore, as adsorption serves as an important connection process within and between many pools of

https://doi.org/10.1346/CCMN.2012.0600401 Published online by Cambridge University Press

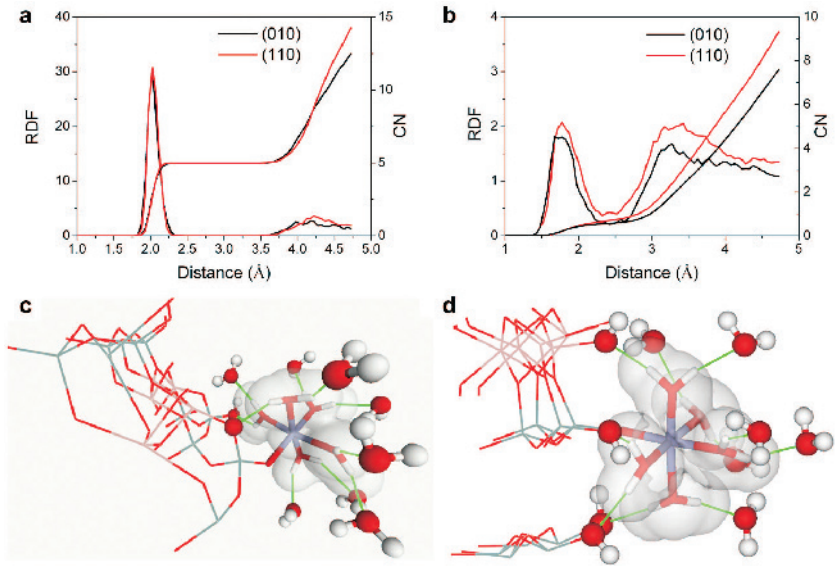

Figure 5. Structures of ≡Si−O complexes. (a) RDF (radial distribution function) and CN (coordination number) for Fe^{2+}−O_{water} in the two ≡Si−O complexes. (b) RDF and CN for H_{1st}−O_{2nd} (oxygen from the second shell around hydrogen from the first shell) in the two ≡Si−O complexes. The shell structures are shown in (c) for the (110) surface and (c) (010) surface. The first shells are illustrated using stick models and covered by contour plots. The second shell molecules are shown using ball-stick models (including surface atoms involved in the coordination spheres). The substrate atoms which did not participate in H-bonding are shown using thin-line models. The green lines denote H bonds, where a H bond is defined by the criterion of O...H distance <2.4 Å and the O−H...O angle ⩾90°. O = red, H = clear, Si = gray, Al = pink, and Fe = dark gray.

Fe in nature (Murad and Fischer, 1988), these findings open the way, at an atomic level, to fill this gap in the geobiochemical cycle of Fe.

ACKNOWLEDGMENTS

The authors acknowledge the National Science Foundation of China (Grant Nos 41002013 and 40973029), PhD Programs Foundation of the Ministry of Education of China (No. 20110091120042), and the Natural Science Foundation of Jiangsu Province (BK2010008), and financial support (No. 2009-II-3) by the State Key Laboratory for Mineral Deposits Research. Liu X. acknowledges the support from Newton International Fellowship program. The authors are grateful to the High Performance Computing Center of Nanjing University for use of the IBM Blade cluster computer system.

REFERENCES

Amira, S., Spångberg, D., Probst, M., and Hermansson, K. (2004) Molecular dynamics simulation of Fe^{2+} (aq) and Fe^{3+} (aq). *Journal of Physical Chemistry B*, **108**, 496−502.

Anderson, R.L., Ratcliffe, I., Greenwell, H.C., Williams, P.A., Cliffe, S., and Coveney, P.V. (2010) Clay swelling − A challenge in the oilfield. *Earth Science Reviews*, **98**, 201−216.

Baeyens, B. and Bradbury, M.H. (1997a) A mechanistic description of Ni and Zn sorption on Na-montmorillonite. 1.Titration and sorption measurements. *Journal of Contaminant Hydrology*, **27**, 199−222.

Bradbury, M.H. and Baeyens, B. (1997b) A mechanistic description of Ni and Zn sorption on Na-montmorillonite. 2. Modeling. *Journal of Contaminant Hydrology*, **27**, 223−248.

Becke, A.D. (1988) Density-functional exchange-energy approximation with correct asymptotic behavior. *Physical Review A*, **38**, 3098−3100.

Bergaya, F., Theng, B.K.G., and Lagaly, G. (2006) *Handbook of Clay Science*. Elsevier, Amsterdam.

Bickmore, B.R., Rosso, K.M., Nagy, K.L., Cygan, R.T., and Tadanier, C.J. (2003) *Ab initio* determination of edge surface structures for dioctahedral 2:1 phyllosilicates: Implications for acid-base reactivity. *Clays and Clay Minerals*, **51**, 359−371.

Bleam, W.F. (1993) Atomic theories of phyllosilicates-quantum-chemistry, statistical-mechanics, electrostatic theory, and crystal-chemistry. *Reviews of Geophysics*, **31**, 51−73.

Bylaska, E.J., Valiev, M., Rustad, J.R., and Weare, J.H. (2007) Structure and dynamics of the hydration shells of the Al^{3+} ion. *Journal of Chemical Physics*, **126**, 104505.

Car, R. and Parrinello, M. (1985) Unified approach for molecular-dynamics and density-functional theory. *Physical Review Letter*, **55**, 2471.

Charlet, L., Silvester, E., and Liger, E. (1998) N-compound reduction and actinide immobilisation in surficial fluids by Fe(II): the surface Fe(III)OFe(II)OH degrees species, as major reductant. *Chemical Geology*, **151**, 85−93.

Churakov, S.V. (2006) *Ab initio* study of sorption on pyrophyllite: Structure and acidity of the edge sites. *Journal of Physical Chemistry B*, **110**, 4135−4146.

Churakov, S.V. (2007) Structure and dynamics of the water films confined between edges of pyrophyllite: A first principles study. *Geochimica et Cosmochimica Acta*, **71**, 1130−1144.

CPMD, Copyright IBM Corp 1990−2006, Copyright MPI für Festkörperforschung Stuttgart 1997−2001.

Cygan, R.T., Liang, J.J., and Kalinichev, A.G. (2004) Molecular models of hydroxide, oxyhydroxide, and clay phases and the development of a general force field. *Journal of Physical Chemistry B*, **108**, 1255−1266.

Cygan, R.T., Greathouse, J.A., Heinz, H., and Kalinichev, A.G. (2009) Molecular models and simulations of layered materials. *Journal of Materials Chemistry*, **19**, 2470–2481.

Den Auwer, C., Simoni, E., Conradson, S., and Madic, C. (2003) Investigating actinyl oxo cations by X-ray absorption spectroscopy. *European Journal of Inorganic Chemistry*, **21**, 3843–3859.

Denecke, M. (2006) Actinide speciation using X-ray absorption fine structure spectroscopy. *Coordination Chemistry Review*, **250**, 730–754.

Ensing, B. and Baerends, E.J. (2002) Reaction path sampling of the reaction between iron(II) and hydrogen peroxide in aqueous solution. *Journal of Physical Chemistry A*, **106**, 7902–7910.

Ensing, B., Buda, F., Blöchl, P.E., and Baerends, E.J. (2002) A Car-Parrinello study of the formation of oxidizing intermediates from Fenton's reagent in aqueous solution. *Physical Chemistry Chemical Physics*, **4**, 3619–3627.

Fredrickson, J.K., Zachara, J.M., Kennedy, D.W., Kukadappu, R.K., Mckinley, J.P., Heald, S.M., Liu, C., and Plymale, A.E. (2004) Reduction of TcO_4^- by sediment-associated biogenic Fe(II). *Geochimica et Cosmochimica Acta*, **68**, 3171–3187.

Gehin, A., Greneche, J.M., Tournassat, C., Brendle, J., Rancourt, D.G., and Charlet, L. (2007) Reversible surface-sorption-induced electron-transfer oxidation of Fe(II) at reactive sites on a synthetic clay mineral. *Geochimica et Cosmochimica Acta*, **71**, 863–876.

Grenthe, I., Stumm, W., Laaksuharju, M., Nilsson, A.C., and Wikberg, P. (1992) Redox potentials and redox reactions in deep groundwater systems. *Chemical Geology*, **98**, 131–150.

Gu, X. and Evans, L.J. (2007) Modelling the adsorption of Cd(II), Cu(II), Ni(II), Pb(II), and Zn(II) onto Fithian illite. *Journal of Colloid and Interface Science*, **307**, 317–325.

Gu, X. and Evans, L.J. (2008) Surface complexation modelling of Cd(II), Cu(II), Ni(II), Pb(II), and Zn(II) adsorption onto kaolinite. *Geochimica et Cosmochimia Acta*, **72**, 267–276.

Gu, X.Y., Evans, L.J., and Barabash, S.J. (2010) Modeling the adsorption of Cd (II), Cu (II), Ni (II), Pb (II) and Zn (II) onto montmorillonite. *Geochimica et Cosmochimica Acta*, **74**, 5718–5728.

Hartman, P. and Perdock, W.G. (1955a) On the relations between structure and morphology of crystals. I. *Acta Crystallographica*, **8**, 49–52.

Hartman, P. and Perdock, W.G. (1955b) On the relations between structure and morphology of crystals. II. *Acta Crystallographica*, **8**, 521–524.

Hartman, P. and Perdock, W.G. (1955c) On the relations between structure and morphology of crystals. III. *Acta Crystallographica*, **8**, 525–529.

Herdman, G.J. and Neilson, G.W. (1992) Ferric ion (Fe(III)) coordination in concentrated aqueous-electrolyte solutions. *Journal of Physics: Condensed Matter*, **4**, 627–638.

Hofstetter, T.B., Neumann, A., and Schwarzenbach, R.P. (2006) Reduction of nitroaromatic compounds by Fe(II) species associated with iron-rich smectites. *Environmental Science & Technology*, **40**, 235–242.

Ikhsan, J., Wells, J.D., Johnson, B.B., and Angove, M.J. (2005) Surface complexation modeling of the sorption of Zn(II) by montmorillonite. *Colloids and Surfaces A*, **252**, 33–41.

Jaisi, D.P., Liu, C., Dong, H., Blake, R.E., and Fein, J.B. (2008) Fe(II) sorption onto nontronite (NAu-2). *Geochimica et Cosmochimica Acta*, **72**, 5361–5371.

Kleinman, L. and Bylander, D.M. (1982) Efficacious form for model pseudopotentials. *Physical Review Letters*, **48**, 1425–1428.

Lagaly, G. (2006) Colloid clay science. Pp. 141–246 in: *Handbook of Clay Science* (F. Bergaya, B.K.G. Theng, and G. Lagaly, editors). Elsevier, Amsterdam.

Lee, C., Yang, W., and Parr, R.G. (1988) Development of the Colle-Salvetti correlation-energy formula into a functional of the electron density. *Physical Review B*, **37**, 785–789.

Liu, X.D. and Lu, X.C. (2006) A thermodynamic understanding of clay-swelling inhibition by potassium ions. *Angewandte Chemie International Edition*, **45**, 6300–6303.

Liu, X.D., Lu, X.C., Wang, R.C., Zhou, H.Q., and Xu, S.J. (2008a) Effects of layer charge distribution on the thermodynamic and microscopic properties of Cs-smectite. *Geochimica et Cosmochimica Acta*, **72**, 1837–1847.

Liu, X.D., Lu, X.C., Wang, R.C., Zhou, H.Q., and Xu, S.J. (2008b) Surface complexes of acetate on edge surfaces of 2:1 type phyllosilicate: Insights from density functional theory calculation. *Geochimica et Cosmochimica Acta*, **72**, 5896–5907.

Liu, X.D., Lu, X.C., Wang, R.C., Meijer, E.J., and Zhou, H.Q. (2012) Atomic-scale structures of interfaces between phyllosilicate edges and water. *Geochimica et Cosmochimica Acta*, **81**, 56–68.

Morel, F.M.M. (1997) Discussion on: "A mechanistic description of Ni and Zn sorption on Na-montmorillonite. Part I: Titration and sorption measurements. Part II: Modeling" by Bart Baeyens and Michael H. Bradbury. *Journal of Contaminant Hydrology*, **28**, 7–10.

Murad, E. and Fischer, W.R. (1988) Geobiochemical cycle of iron. Pp. 1–18 in: *Iron in Soils and Clay Minerals* (J.W. Stucki, B.A. Goodman, and U. Schwertmann, editors). D. Reidel, Dordrecht, The Netherlands.

Peretyazhko, T., Zachara, J.M., Heald, S.M., Jeon, B.-H., Kukkadapu, R.K., Liu, C., Moore, D., and Resch, C.T. (2008) Heterogeneous reduction of Tc(VII) by Fe(II) at the solid-water interface. *Geochimica et Cosmochimica Acta*, **72**, 1521–1539.

Remsungnen, T. and Rode, B.M. (2003) QM/MM molecular dynamics simulation of the structure of hydrated Fe(II) and Fe(III) ions. *Journal of Physical Chemistry A*, **107**, 2324–2328.

Schultz, C. and Grundl, T. (2004) pH dependence of ferrous sorption onto two smectite clays. *Chemosphere*, **57**, 1301–1306.

Sposito, G. (1984) *The Surface Chemistry of Soils*. Oxford University Press, New York.

Sposito, G., Skipper, N.T., Sutton, R., Park, S.-H., Soper, A.K., and Greathouse, J.A. (1999) Surface geochemistry of the clay minerals. *Proceedings of the National Academy of Sciences*, **96**, 3358.

Stucki, J.W. (2006) Properties and behavior of iron in clay minerals. Pp. 423–476: *Handbook of Clay Science* (F. Bergaya, B.G.K. Theng, and G. Lagaly, editors). Elsevier, Amsterdam.

Troullier, N. and Martins, J.L. (1991) Efficient pseudopotentials for plane-wave calculations. *Physical Review B*, **43**, 1993–2006.

Um, W., Chang, H.S., Icenhower, J.P., Lukens, W.W., Serne, R.J., Qafoku, N.P., Westsik, J.H., Buck, E.C., and Smith, S.C. (2011) Immobilization of 99-Technetium (VII) by Fe(II)-goethite and limited reoxidation. *Environmental Science & Technology*, **45**, 4904–4913.

Viani, A., Gaultieri, A.F., and Artioli, G. (2002) The nature of disorder in montmorillonite by simulation of X-ray powder patterns. *American Mineralogist*, **87**, 966–975.

White, G.N. and Zelazny, L.W. (1988) Analysis and implications of the edge structure of dioctahedral phyllosilicates. *Clays and Clay Minerals*, **36**, 141–146.

(*Received 20 January 2012; revised 2 July 2012; Ms. 645; AE: J.W. Stucki*)